Proceedings of the 28th IEEE
EMBS Annual International Conference
New York City, USA, Aug 30-Sept 3, 2006

Transmural electrophysiological heterogeneities in action potential duration increase the upper limit of vulnerability

T. Maharaj, B. Rodriguez, R. Blake, N.A. Trayanova, D.J. Gavaghan

***Abstract*—Transmural dispersion in action potential duration (APD) has been shown to contribute to arrhythmia induction in the heart. However, its role in termination of lethal arrhythmias by defibrillation shocks has never been examined. The goal of this study is to investigate how transmural dispersion in APD affects cardiac vulnerability to electric shocks, in an attempt to better understand the mechanisms behind defibrillation failure. This study used a three-dimensional, geometrically accurate finite element bidomain rabbit ventricular model. Transmural heterogeneities in ionic currents were incorporated based on experimental data to generate the transmural APD profile recorded in adult rabbits during pacing. Results show that the incorporation of transmural APD heterogeneities in the model causes an increase in the upper limit of vulnerability from 26.7V/cm in the homogeneous APD ventricles to 30.5V/cm in the ventricles with heterogeneous transmural APD profile. Examination of shock-end virtual electrode polarisation and postshock electrical activity reveals that the higher ULV in the heterogeneous model is caused by increased dispersion in postshock repolarisation within the LV wall, which increases the likelihood of the establishment of intramural re-entrant circuits.**

***Keywords*—cardiac vulnerability, electrophysiological heterogeneities, defibrillation, bidomain simulations**

I. Introduction

EXPERIMENTAL and theoretical studies in both isolated ventricular tissue [1], [2], [18], [21] and single myocytes [20] have proved that transmural dispersion in action potential duration (APD) exists, which results from changes in ionic properties in the depth of the ventricular wall. In particular, three layers of functionally-different cell types have been identified, namely the epicardial, endocardial and midmyocardial layers. Experimental and theoretical studies have proved that transmural dispersion in APD in the ventricles, which varies with age [7] and animal species [4], [7], [13], [14] may modulate the arrhythmogenic substrate [23] and thus could alter defibrillation efficacy. However, the role of transmural heterogeneities in the mechanisms underlying defibrillation failure is unknown. The goal of this study is to investigate how transmural dispersion in APD affects cardiac vulnerability to electric shocks in an attempt to better understand defibrillation failure.

Manuscript received April 3, 2006. This work was supported by a Rhodes scholarship to T. M., the EPSRC-funded Integrative Biology e-Science pilot project (ref no: GR/S72023/01), by the EU BioSim Grant (005137) and by AHA Established Investigator Award (N.T.), and the grant HL63195 from NIH (N.T).

T. Maharaj, B. Rodriguez and D. Gavaghan are with the Computing Laboratory, Oxford, UK (corresponding author e-mail: thum@comlab.ox.ac.uk). R. Blake and N. Trayanova are with Tulane University, New Orleans, LA, USA.

II. Methodology

A. Computational model

We used an anatomically based rabbit ventricular model [16] that incorporates realistic fiber orientation, and includes representation of the perfusing bath and the fluid filled ventricular cavities. Electrical activity in the myocardium was represented by the bidomain equations, which were solved using a semi-implicit finite element method as was previously described in [15].

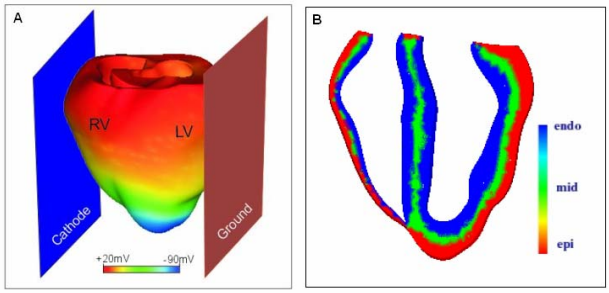

Fig. 1. A) Anterior view of the rabbit ventricular model with shock electrodes showing the epicardial transmembrane potential distribution. LV= left ventricle; RV= right ventricle. B) Illustration of the cell types that have been incorporated into the ventricular model.

Shocks were applied via two large planar electrodes located at the boundaries of the perfusing bath (Fig. 1A). The electrode near the right ventricle (RV) was the cathode, and the one near the left ventricle (LV) the grounding electrode. The Luo-Rudy dynamic model [8] [19], modified for defibrillation [3] was used to represent the kinetics of ionic currents in both a homogeneous APD model (membrane kinetics as in Ashihara and Trayanova [3]) and in a model that incorporates transmural heterogeneities in the transient outward current (I_{to}) and the slow delayed rectifier potassium current (I_{Ks}). Transmural heterogeneities in I_{to} and I_{Ks} were incorporated based on experimental data to generate the transmural APD profile recorded in adult rabbits [7] during pacing stimulation. Endocardial, epicardial and midmyocardial layers were represented with relative thicknesses of 3:3:2, ie. the walls of the ventricles were made up of 37.5% endocardial tissue, 37.5% epicardial tissue and 25% midmyocardial tissue [12]. Table 1 presents the values of the maximum conductances of I_{to} [5]-[6] and I_{Ks} [24], [12], in each layer.

TABLE I
MODEL PARAMETERS

	Epicardium	Midmyocardium	Endocardium
G_{To} (mS/μF)	0.5	0.2125	0
G_{Ks} (mS/μF)	0.75	0.25	0.3

B. Vulnerability grids

The rabbit ventricular model was paced at the apex at a basic cycle length of 250ms [9]. After 7 paced beats, 8ms truncated exponential monophasic shocks of varying strengths (3.81 - 30.46 V/cm) and coupling intervals (CI) between 100 and 200ms were applied via large planar electrodes located at the boundaries of the bath (Fig. 1). Vulnerability grids were constructed by examining the outcome of shocks. An arrhythmia was defined as sustained if two or more heart beats were induced after the application of the shock [10]. The upper limit of vulnerability (ULV) was determined in both models as the highest shock strength above which sustained re-entry was no longer induced. Shock strengths refer to the leading edge value of the applied electric field.

III. RESULTS

A. Transmural dispersion in APD

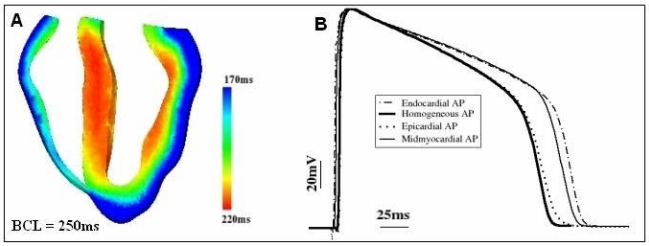

Fig. 2. Dispersion in the action potential duration. A) APD distribution in a transmural slice through the heterogeneous ventricles showing an APD map measured at 90% repolarisation. B) Time course of the AP in the homogeneous model (bold solid line) and in the epicardial (.), midmyocardial (-) and endocardial (-.-) layers within the LV wall in the heterogeneous model.

Fig. 2A illustrates the APD distribution across a transmural slice of the heterogeneous model. Action potential duration was measured at 90% repolarisation. Consistent with previous experimental and theoretical studies [7, 11], transmural heterogeneities in I_{to} and I_{Ks} result in a marked dispersion of APD across the LV, RV walls and the septum with APDs ranging from 170ms to 220ms. The longest APDs were recorded in the septum and in the endocardium of the LV free wall.

Fig. 2B illustrates the time course of the action potential in a LV node of the homogeneous ventricular model (bold solid line) and in an epicardial node (… line), a midmyocardial node (– line) and a endocardial node (-.- line) of the heterogeneous ventricular model. The epicardial, midmyocardial and endocardial nodes were taken from the middle of each respective layer in the LV. Fig. 2B shows that APD is shorter in the midmyocardium than in the endocardium, in spite of the fact that G_{Ks} (defined in Table 1) is lower in the midmyocardium than in the endocardium. This modulation of APD is due to the electrotonic interaction between the three layers that acts to shorten the midmyocardial AP and to prolong the epicardial and endocardial APs [11, 21].

B. Role of transmural heterogeneities in cardiac vulnerability to electric shocks

The simulation results show that ULV is 26.67V/cm for the homogeneous model and increases to 30.46V/cm with inclusion of transmural dispersion of APD in the ventricles.

In order to elucidate the mechanisms responsible for this increase in ULV, we analyse the effect of incorporating transmural heterogeneities in the pre-shock state of the tissue, the virtual electrode polarisation (VEP) [22] and the postshock electrical activity for various shock strengths and CIs.

Fig. 3 shows the transmembrane potential distribution at the time of shock delivery, at shock end and following a shock of 30.5V/cm strength, applied at CI=140ms to the homogeneous (Fig.3A) and heterogeneous APD (Fig.3B) ventricles. This episode was chosen as CI=140ms is a CI at which the ULV occurs in both the homogeneous and heterogeneous models and for this episode, an arrhythmia was induced in the heterogeneous model but not in the homogeneous model. Thus, by examining the differences in the electrical activity between both models, it is possible to determine the mechanism underlying the increase in ULV.

Fig. 3 shows that the transmembrane potential distribution at the time of shock delivery and at the end of the shock is similar in both models (Fig. 3, preshock and 0ms panels). Consistent with experimental optical mapping recordings [22], two main areas of opposite polarisation are induced on the epicardium by the shock: the RV epicardium is positively polarised while the LV epicardium is negatively polarised (Fig. 3, 0ms panels). In contrast to the surface view, the transmural views in the 0ms panels in Fig. 3 show a complex distribution of transmembrane potential in the depth of the ventricular wall, consistent with previous studies [10].

Following the end of the shock, similar behaviour occurs in both models: a wavefront propagates from apex to base within the LV wall (Fig. 3, 20ms panels).

However, a big difference between the homogeneous and the heterogeneous ventricular models arises in the encircled areas in Fig, 3, 20ms panels, which eventually determines the outcome of the shock. As postshock propagation is slower in the heterogeneous APD model than in the homogeneous APD model, at 20ms postshock, the extent of the excitable area in the heterogeneous model (Fig. 3B, 20ms panel) is larger than that in the homogeneous model (Fig. 3B, 20ms panel). This finding has been quantified by determining the percent of myocardial nodes experiencing potentials below -50mV in the encircled areas (Fig. 3A and 3B, 20ms panels). At 20ms postshock, the amount of

myocardial nodes in the encircled area, with Vm<-50mV is 27.24% in the homogeneous model as compared to 33.42% in the heterogeneous model, indicating that there is a larger excitable area ahead of the wavefront in the LV free wall in the heterogeneous than in the homogeneous model.

As shown in Fig. 3A, in the homogeneous model, propagation quickly traverses the small postshock excitable gap located in the LV wall (Fig.3A, 30ms panel) and shortly thereafter the wave is blocked surrounded by refractory tissue and no arrhythmia is induced (Fig 3A, 60ms, 100ms panels).

In contrast, in the heterogeneous model, following shock end, postshock propagation traverses the postshock excitable area located within the LV free wall. Meanwhile, tissue in the LV epicardium recovers, providing a pathway for propagation. Thus, the postshock wavefront breaks through to the epicardial surface at 50ms postshock (Fig. 3B. 50ms panel, encircled area) and then continues towards the septum and the RV tissue, which have already recovered from shock-induced positive polarisation (Fig. 3B, 100ms panel). As shown in Fig. 3B, the wavefront re-enters through the midmyocardium of the LV free wall, ultimately, leading to the establishment of an intramural re-entrant circuit.

Thus, as shown in Fig. 3, the increased ULV in the heterogeneous APD ventricles compared to the homogenous APD ventricles, results from increased dispersion of refractoriness in the LV free wall, and in particular from the fact that the LV free wall epicardial tissue repolarises faster than the endocardium or midmyocardium (Fig. 2A). This enables the propagation of the wavefront on the epicardial surface (Fig. 3B, 60ms panel) and the establishment of a re-entrant circuit.

IV. Conclusion

This study used a sophisticated computer model of stimulation/defibrilation, to provide mechanistic insight into the role of transmural electrophysiological heterogeneities in cardiac vulnerability to electric shocks. As demonstrated here, bidomain computer simulations have the ability to faithfully predict the VEP pattern and postshock electrical activity within the depths of the ventricular wall, which is not achievable by any experimental techniques thus far. The insight provided by the simulations revealed that the elevation in ULV in the heterogeneous ventricles stems from increased transmural dispersion in postshock refractoriness within the LV free wall.

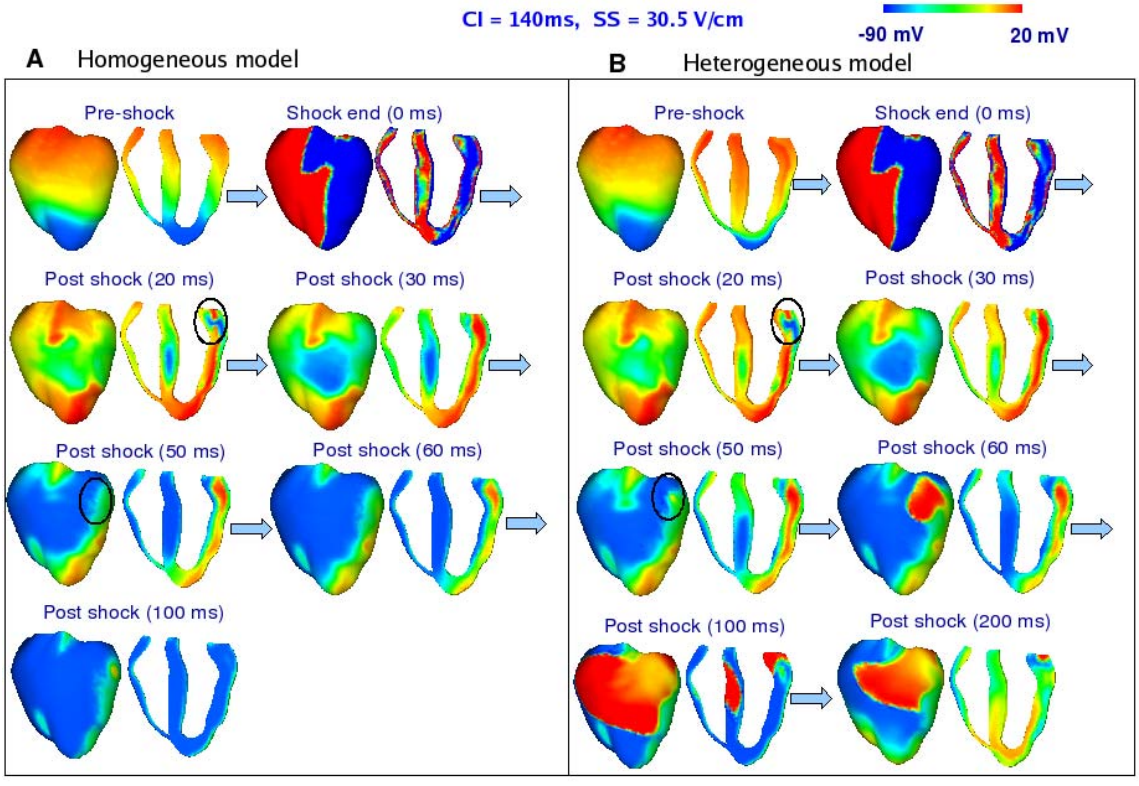

Fig. 3. Transmembrane potential distribution: pre-shock (epicardial and transmural views), at shock end (epicardial and transmural views) and the evolution of electrical activity after the shock (epicardial and transmural views) for shock strength 30.5 V/cm applied at CI = 140ms. A) corresponds to the homogeneous ventricular model, and B) to the heterogeneous ventricular model. Colour scale is saturated, ie. transmembrane potential above 20mV and below −90mV appear red and blue, respectively.

REFERENCES

[1] C. Antzelevitch, W Shimizu, GX Yan, S. Sicouri, J. Weissenburger, VV. Nesterenko, A. Burashnikov, J. Di Diego, J Saffitz, and GP. Thomas, "The M cell: its contribution to the ECG and to normal and abnormal electrical function of the heart." *J Cardiovasc Electrophysiol.*, pp. 1124-52, 1999.

[2] C. Antzelevitch, G.X. Yan, W. Shimizu, and A. Burashnikov, "Electrical heterogeneity, the ECG, and cardiac arrhythmias, From Cell to Bedside," W.B. Saunders Company, Philadelphia, 1999.

[3] T. Ashihara and N. A. Trayanova, "Asymmetry in membrane responses to electric shocks: Insights from bidomain simulations," *Biophysical Journal*, pp. 2271-2282, 2004.

[4] E. Drouin, F. Charpentier, C. Gauthier, K. Laurent, and H. Le Marec, "Electrophysiologic characteristics of cells spanning the left ventricular wall of human heart: evidence for presence of M cells," *J Am Coll Cardiol*., pp.185-192, 1995.

[5] R. Dumaine, J. A. Towbin, P. Brugada, M. Vatta, D. V. Nesterenko, V. V. Nesterenko, J. Brugada, R. Brugada, and C. Antzelevitch, "Ionic mechanisms responsible for the electrocardiographic phenotype of the Brugada syndrome are temperature dependent," *Circ. Res.*, pp. 803-809,1999.

[6] K. Gima and Y. Rudy, "Ionic current basis of electrocardiographic waveforms: A model study," *Circ Res*, pp. 889–896, 2002.

[7] S.F. Idriss and P. D. Wolf, "Transmural action potential repolarisation heterogeneity develops postnatally in the rabbit," *J. Cardiovas Electrophysiol*, pp. 795-801, 2004.

[8] C.H. Luo and Y. Rudy, "A dynamic model of the cardiac ventricular action potential: I. Simulations of ionic currents and concentration changes," *Circ. Res.*, pp.1071-1096, 1994.

[9] R. A. Malkin, S. F. Idriss, R. G.Walker, and R. E. Ideker, "Effect of rapid pacing and t-wave scanning on the relation between the defibrillation and upper-limit-of-vulnerability dose-response curves," *Circulation*, pp.1291-1299, 1995.

[10] B. Rodriguez, L. Li, JC. Eason, IR. Efimov, and N. Trayanova, "Differences between left and right ventricular chamber geometry affect cardiac vulnerability to electric shocks," *Circ Res*, pp.168, 2005.

[11] K. J. Sampson and C. S. Henriquez, "Simulation and prediction of functional block in the presence of structural and ionic heterogeneity," *Am J Physiol*, pp. 2597-2603, 2001.

[12] J. J. Saucerman, S. N. Healy, M. E. Belik, J. L. Puglisi, and A. D. McCulloch, "Proarrhythmic consequences of a KCNQ1 AKAP-binding domain mutation computational models of whole cells and heterogeneous tissue," *Circ. Res.*, pp. 1216, 2004.

[13] S. Sicouri and C. Antzelevitch, "A subpopulation of cells with unique electrophysiological properties in the deep subepicardium of the canine ventricle: the M cell," *Circ Res*, pp.1729-1741, 1991.

[14] S. Sicouri, M Quist, and C. Antzelevitch, "Evidence for the presence of M cells in the guinea pig ventricle," *J Cardiovasc Electrophysiol.*, pp. 503-511, 1996.

[15] N. Trayanova, J. Eason, and F. Aguel, "Computer simulations of cardiac defibrillation: A look inside the heart," *Computer Visual Science*, pp. 259 – 270, 2002.

[16] FJ. Vetter and AD. McCulloch, "Three-dimensional analysis of regional cardiac function: a model of rabbit ventricular anatomy," *Prog Biophys Mol Biol.*, pp. 157-183, 1998.

[17] P. C. Viswanathan, R. M. Shaw, and Y. Rudy, "Effects of IKr and IKs heterogeneity on action potential duration and its rate dependence a simulation study," *Circulation*, pp. 2466-2474 1999.

[18] G. X. Yan, S. J. Rials, Y. Wu, T. Liu, X. Xu, R. A. Marinchak, and P. R. Kowey, "Ventricular hypertrophy amplifies transmural repolarization dispersion and induces early afterdepolarization," *Am J Physiol Heart Circ Physiol.*, pp. 1968-1975, 2001.

[19] C.H. Luo, Y. Rudy, "A dynamic model of the cardiac ventricular action potential. II. Afterdepolarizations, triggered activity, and potentiation.,"*Circ Res,* pp. 1097-1113, 1994.

[20] MA McIntosh, SM Cobbe, GL. Smith, "Heterogeneous changes in action potential and intracellular Ca2+ in left ventricular myocyte sub-types from rabbits with heart failure," *Cardiovasc Res.,* pp. 397-409, 2000.

[21] G-X Yan, W. Shimizu, and C. Antzelevitch, "Characteristics and distribution of M cells in arterially perfused canine left ventricular wedge preparations," *Circulation*, pp.1921-1927, 1998.

[22] I. R. Efimov, F. Aguel, Y. Cheng, B. Wollenzier, and N. Trayanova, **"**Virtual electrode polarization in the far field: implications for external defibrillation," *Am J Physiol Heart Circ Physiol*, pp.1055-1070, 2000.

[23] C. Antzelevitch, J. Fish, "Electrical heterogeneity within the ventricular wall," *Bas Res Cardiol.,* pp.517 – 527, 2001.

[24] X. Xu, S. J. Rials, Y. Wu, J. J. Salata, et al. "Left Ventricular Hypertrophy Decreases Slowly but Not Rapidly Activating Delayed Rectifier Potassium Currents of Epicardial and Endocardial Myocytes in Rabbits," *Circulation,* pp. 1585-1590, 2001.